Available online at www.sciencedirect.com
SCIENCE DIRECT
Journal of Molecular Catalysis A: Chemical 251 (2006) 54–65
JOURNAL OF MOLECULAR CATALYSIS A: CHEMICAL
www.elsevier.com/locate/molcata

Basis for specificity in methane monooxygenase and related non-heme iron-containing biological oxidation catalysts

J. Zhang, H. Zheng, S.L. Groce, J.D. Lipscomb *

Department of Biochemistry, Molecular Biology, and Biophysics and the Center for Metals in Biocatalysis, University of Minnesota, Minneapolis, MN 55455, USA

Available online 10 March 2006

Abstract

Biological systems activate O_2 using many mechanisms, but in nearly all cases, the activation process is regulated to assure specificity. The nature of these regulatory aspects of the reaction must be understood before the true nature of the underlying chemistry can be described with certainty. Most metal-containing oxygenases utilize amino acids in the second sphere and beyond to regulate the O_2 activation reaction. One example of this is seen in the mechanism of substrate selectivity by methane monooxygenase. The regulatory protein MMOB binds to the active site-containing MMOH and appears to create a pore sized for methane into the active site. This controls access and therefore the preferred substrate. Also, the complex appears to cause quantum tunneling to dominate in C–H bond cleavage reaction for methane, selectively increasing the rate for this substrate. Both effects can be altered by mutagenesis of MMOB, potentially broadening the substrate range of the enzyme. Second sphere effects are also important in determining the position of ring cleavage for catecholic ring cleaving dioxygenases. Intermediates throughout the catalytic cycle of homoprotocatechuate 2,3-dioxygenase can be detected by using the chromophoric substrate 4-nitrocatechol (4NC). Upon mutation of the second sphere residue histidine 200 to asparagine (H200N), the rate of reaction of the Fe-oxy intermediate is greatly slowed, allowing its detection for the first time when using either 4NC or the natural substrate 3,4-dihydroxyphenylacetate (HPCA). HPCA cleavage occurs in the usual proximal extradiol position by this mutant, but 4NC is oxidized to the quinone without ring cleavage. Use of the alternative substrate 2,3-dihydroxybenzoate results in distal extradiol cleavage for the wild type enzyme, but intradiol cleavage for the H200-phenylalanine mutant. Thus, control of the second sphere allows the enzyme to design a specific catalyst that gives only one of the four potential types of products. This insight can be used to design specific enzyme oxidation catalysts.

Keywords: Methane monooxygenase; Dioxygenase; Regulation; O_2 activation; Second sphere effects

1. Introduction

Metalloenzymes that activate molecular oxygen possess great potential as catalysts for specific oxidation reactions and as guides for the development of efficient small molecule catalysts [see for example [1–3]]. Studies of the mechanisms of various biological catalysts is particularly useful in the design of small molecule catalysts, especially if the chemical nature of specific intermediates in the catalytic cycle of the enzyme can be detected and characterized. Indeed, most of the focus of ongoing biomimetic and bio-inspired synthetic approaches is on reproducing some structural aspect of the metal center or the chemical nature of one of the reaction cycle intermediates. This approach has met with considerable success, and many small molecule catalysts capable of relatively specific hydroxylation, dihydroxylation, *N*-oxidation, desaturation and other types of oxidation reactions typical of enzyme oxidants are now available [see for example [4,5]]. However, there is another level of sophistication in biological oxidation catalysts that has, for the most part, not been incorporated into small molecule catalysts. This derives from the complex structure of the biocatalyst and can generally be referred to as the "second sphere", although for our purposes we will broaden this definition to include all elements of structure that affect the active site beyond the direct ligands to the metal.

It is useful to consider some of the forces that shape the evolution of a metalloenzyme active site. These differ in many respects from the considerations typically used to define the criteria for a good small molecule catalyst. First, nature values specificity above rate. Rate can be adjusted at will by a biological system by controlling the level of expression of the enzyme, but generation of the wrong product is a dead end because there are no

* Corresponding author. Tel.: +1 612 625 6454; fax: +1 612 624 5121.
E-mail address: lipsc001@umn.edu (J.D. Lipscomb).

1381-1169/$ – see front matter © 2006 Elsevier B.V. All rights reserved.
doi:10.1016/j.molcata.2006.02.023

downstream enzymes to deal with such molecules. As a result, the optimal chemical mechanism judged by its rate is often not the route chosen by nature. Second, metal ligand asymmetry caused by ligand selection and distortions in the second sphere is used routinely by nature to adapt the same type of metal site for numerous tasks and to generate stereo- and regio-specific products. Third, nature tightly controls the supply of protons and electrons in terms of quantity, spatial point of introduction in the active site, and temporal point of introduction in the reaction cycle. Fourth, nature can strongly influence reactions by placing hydrogen bonding, polarizing, or acid/base catalysts at specific locations in the second sphere. Finally, nature can rigorously control access to the active site. As shown below, access limitations can easily occur at the level of single methyl group.

At the outset, the study of an enzyme mechanism is generally undertaken using the same tools as the chemist uses to investigate the reaction of a small molecule catalyst, namely, kinetics, spectroscopy, and diagnostic reactions. However, the special properties of a biological catalyst described above often complicate the investigation, sometimes misleading the investigator. This is particularly true if access is used to regulate a biological reaction, but most of the other types of second sphere effects can also lead a mechanistic study down the wrong track. Here, two examples of studies of oxygenase enzymes are used to illustrate this point. In the first, the special control of access into the active site of methane monooxygenase (MMO) is discussed in the context of mechanism and regulation. Second, the influence of the second sphere structure of aromatic ring cleaving dioxygenases is used to show how nature can make an inherently nonspecific reaction unerringly specific.

2. Access and regulation in the methane monooxygenase system

2.1. The MMO system

The soluble form of MMO (sMMO) is isolated from methanotrophic bacteria as a three protein component system illustrated in Fig. 1 [6]. A reductase (MMOR) contains an Fe_2S_2 cluster and a FAD cofactor that act to transfer two reducing equivalents from NADH to the hydroxylase component (MMOH). This component has an $(\alpha\beta\gamma)_2$ subunit structure and harbors the active site in the α-subunit. The active site contains a bis-μ-hydroxo-bridged dinuclear iron cluster, which is known to activate molecular oxygen and transfer one atom to substrates. The third component termed "B" (MMOB) contains no metals or cofactors. It forms a tight complex with the α-subunits of MMOH. Importantly, for interpretation of the results presented here, the X-ray crystal structure of MMOH, a portion of which is shown in Fig. 2, reveals that the active site is buried with no obvious channel from bulk solution [7,8]. Consequently, MMOB must be at least 12 Å from the diiron cluster in the binary complex. Nevertheless, the MMOH–MMOB complex shows greatly different reactivity than the MMOH alone. For example, the rate of turnover is increased 150-fold and rate constant for O_2 binding is increased 1000-fold in the binary complex [9]. The regiospecificity for hydroxylation of complex, adventitious substrates is

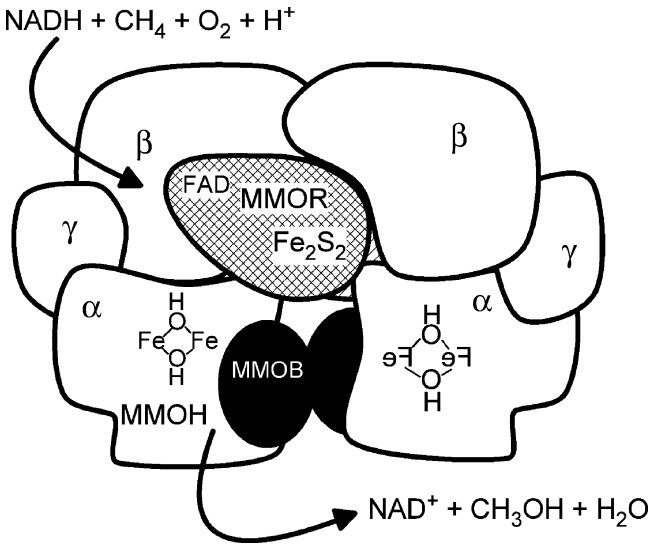

Fig. 1. The three protein components of the soluble methane monooxygenase system.

drastically altered when MMOB is bound [10]. Moreover, the spectroscopic features of the diiron cluster are changed, and its redox potential is shifted by over −130 mV [11,12]. These and other observations show that the effects of MMOB binding to the MMOH surface are transmitted to the interior in some manner. We believe that this is a manifestation of the regulatory mechanism of sMMO.

Why does sMMO need a regulatory mechanism? As the name implies, methanotrophs grow only using methane as a substrate. Through the catalytic action of sMMO, methane is oxidized to methanol with 100% efficiency with no over-oxidation [13]. Methanol is then further oxidized by other enzymes in two-electron steps to CO_2. During these three further oxidation steps, the organism recovers six electrons for every two invested in the sMMO reaction. Methanotrophs have no enzyme pathways for other substrates. Thus, they must find a way to selectively oxidize the substrate with the most stable C–H bonds in what is often the presence of hundreds of other potential substrates with weaker C–H bonds. This is not to say that sMMO cannot catalyze oxidation of these other substrates. Indeed, hundreds of other substrates are known and dozens of different types of oxidation reactions are catalyzed [3,14]. However, these adventitious substrates are oxidized much slower than their relative C–H bond strength would indicate [15]. The oxidation of these substrates is useful to the chemist, if not the bacteria. It allows the enzyme to be used in a wide variety of degradation tasks by environmental scientists and potentially as a synthetic tool in industry [16,17]. Moreover, the oxidation of many types of probe molecules has proven to be a valuable tool in assessing the molecular mechanism of catalysis [see for example [18–22].

2.2. The MMOH catalytic cycle

MMOH is colorless in the visible, and the spin coupling of the iron atoms in the diiron cluster make it EPR silent in the rest-

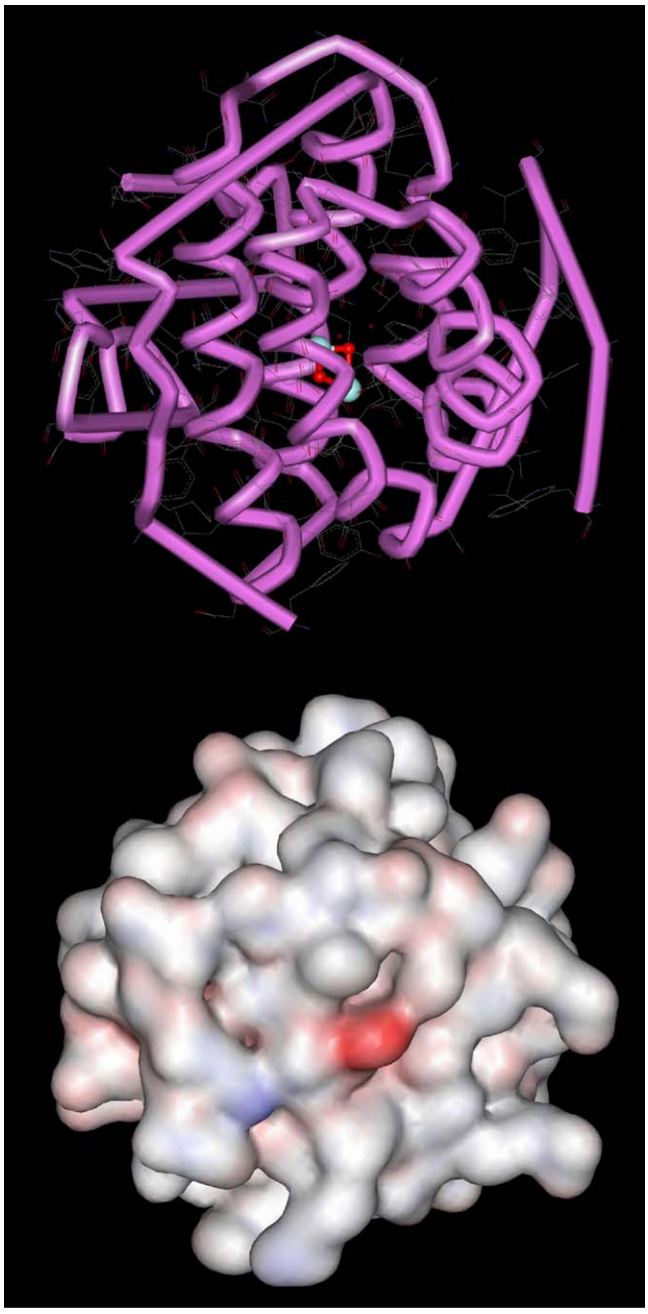

Fig. 2. Structure of a 30 Å diameter sphere surrounding the active site diiron cluster of MMOH. *Top*: The diiron cluster is buried in a 4-helix bundle 12 Å below the surface of the α-subunit. *Bottom*: When the space occupied by amino acids is filled, the cluster is not visible from any angle, suggesting that there is no entry channel.

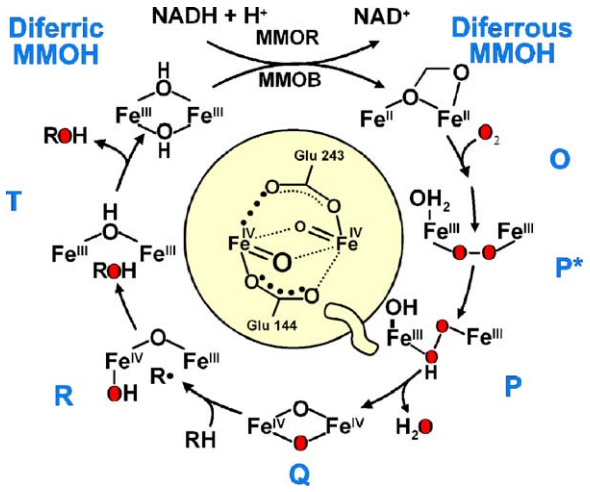

Fig. 3. Proposal for the catalytic cycle of sMMO. The detectable transient intermediates of the cycle depicted as letters next to the hypothetical structure of the intermediate at the diiron cluster. The proposed structure for compound Q based on spectroscopic studies is shown in the center.

ing state [23]. Fortunately, some of the intermediates that occur during the catalytic cycle acquire unique spectroscopic properties that allow them to be detected. Thus, it has been possible to follow a single turnover of the MMOH in the presence of a stoichiometric amount (per active site) of MMOB after reducing the cluster to the diferrous state and rapidly admitting O_2 [24].

The current view of the catalytic cycle is illustrated in Fig. 3. It begins by O_2 binding to the enzyme but not to the iron to yield an "oxygen" intermediate termed O [9,24]. Then O_2 binds to the cluster to yield a superoxo- or bridging peroxo-adduct termed P^* [25]. With the successive input of two protons [26], P^* converts to the hydroperoxy complex P [24,27], and then the unique bis-μ-oxo dinuclear Fe(IV) compound Q [24]. Q has not been found in any other biological system and references to multinuclear Fe(IV) complexes are only beginning to appear in the chemical literature [28]. Our experiments have shown that it is capable of reacting with methane and other substrates to yield the product bound in the active site (compound T) [24]. T then releases product into solution in what is usually the rate-limiting step in turnover. An important characteristic of Q is that it has a fairly intense yellow chromophore, so that its reaction with substrates can be directly monitored in real time. This is the first time that it has been possible to observe the discrete reaction in which oxygen is transferred to substrate in a metallo-monooxygenase. Q is electronically equivalent to the elusive compound **I** of cytochrome P450 monooxygenase [29], which cannot be directly monitored, although it has recently been structurally characterized [30]. Thus, MMOH provides our first opportunity to study the chemistry of high valent metallo-intermediates in oxygenases. These are the engines for the most difficult oxidation chemistry in biology.

Another useful property of the Q reaction is that, in the absence of substrate, the formation rate is faster than the decay rate constant. This means that Q builds up in the reaction mixture and can be trapped in high yield for spectroscopic characterization [31]. X-ray absorption and Mössbauer studies interpreted in the light of model compounds showed that Q has a diamond core structure with two asymmetrically bridging oxo-groups between the two Fe(IV)s as illustrated in the center of Fig. 3 [32]. This can be thought of as two Fe(IV)-oxo units joined head to tail. As substrates are added, the formation rate of Q is unchanged, but the decay rate constant increases linearly with substrate concentration [24]. As illustrated in Fig. 4, the slope of the resulting plot depends strongly on the substrate type, reinforcing the idea that Q reacts directly with hydrocarbons.

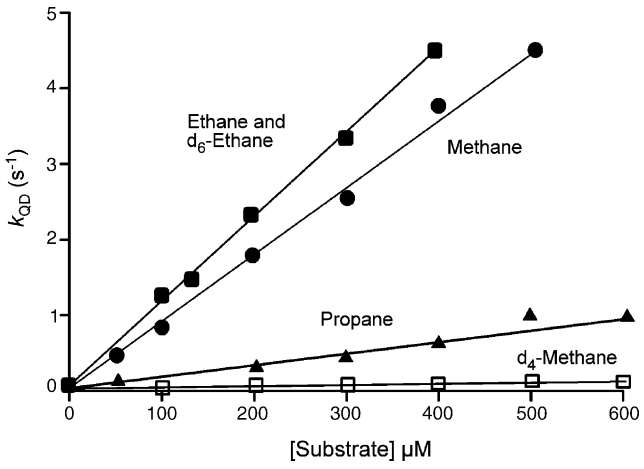

Fig. 4. Linear dependence of the decay rate constant of Q on substrate concentration.

2.3. Proposals for the mechanism of C–H bond cleavage

The ability to directly observe monooxygenase chemistry for an array of substrates, and the availability of high resolution structures, has led to numerous proposals for the mechanism of C–H bond activation, some of which are illustrated in Fig. 5 [6,33]. The mechanism illustrated in Fig. 3 and the Fig. 5iii is similar to that proposed for cytochrome P450, termed oxygen rebound [29]. In this mechanism, Q abstracts a hydrogen atom from the substrate to yield a formal cluster-bound hydroxyl radical and a substrate radical in the active site. Recombination of the radicals yields the product. This mechanism is supported by numerous experiments that demonstrate the presence of a radical or a cation intermediate in the active site. For example, *R* or *S* 1-[^{2}H, ^{3}H]-ethane is oxidized to labeled ethanol that is 35% racemerized indicative of an intermediate [18].

While the chiral ethane experiment just cited appears at first to be definitive, the fact that the racemerization is not complete suggests that any intermediate must live only a few hundred femtoseconds, not long enough for physical motion inherent in the rebound mechanism. It was suggested that the reaction is really concerted with the loss of chirality due to partial radical character of the transition state [22]. This was experimentally supported by the observation that some ultrafast radical clock substrates did not rearrange, suggesting that no discrete radical is formed. Computational results first supported this mechanism, but they gradually migrated to a middle ground between the concerted and rebound mechanism as the size of the computation model increased [34]. The current proposal (Fig. 5iv) is for a bound radical mechanism in which complete C–H bond breaking occurs, but the products remain associated, so that the rebound occurs without significant molecular motion.

A different type of mechanistic proposal derives from another computational approach. It was proposed that the methane carbon binds directly to Fe(IV) of the cluster, as shown in Fig. 5ii, so that the lower symmetry of the molecule allows easier C–H bond cleavage [35]. The hydrogen is retained on the oxygen bridge so the formation of methanol can occur without a diffusible intermediate. In the case of chiral ethane, pseudo-rotation on the iron-bound carbon would lead to loss of chirality.

Finally, it has been proposed that the hydroperoxy intermediate P may be the reactive species in some cases by transferring an OH+ to the substrate followed by loss of water to yield a cation (Fig. 5i) [36]. This mechanism is supported by the observation that there are many cases in which a cation intermediate is indicated in diagnostic sMMO catalyzed reactions [19,21,36,37]. However, we have speculated that these intermediates arise because the Fe(III)Fe(IV) intermediate that would result from hydrogen atom abstraction by Q is still sufficiently oxidizing to abstract a second electron [21,38].

In principle, it should be possible to test the rebound mechanism by showing that the log rate constant for Q decay varies inversely with the C–H bond dissociation energy of the substrate. Also, there should be kinetic isotope effect (KIE) for this step if deuterated substrates are used. In fact, the hydrocarbons that react fastest with Q are those with the strongest bonds, ethane and methane [25]. There is a very large, primary KIE of 50 for the methane reaction [39]. However, there is no observed KIE for any other substrate, including ethane [25]. These observations may indicate that the rebound mechanism is not correct. On the other hand, they may indicate that the true chemistry of sMMO is masked by one of the best examples of nature using access to control a biological system.

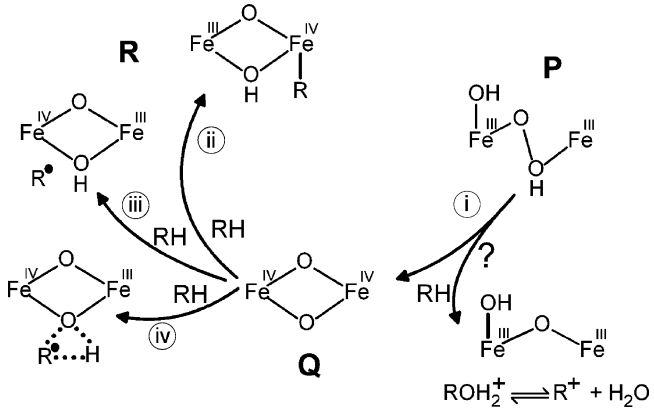

Fig. 5. Summary of the general types of mechanisms proposed for the reaction of sMMO with hydrocarbon substrates.

2.4. The steps in the Q reaction

The linearity of the plot of the Q decay rate constant versus substrate concentration shown in Fig. 4 suggests that this is a second order reaction. When the data is collected over a range of temperature for most substrates (for example, Fig. 6, dashed line), linear Arrhenius plots are observed supporting the idea that this is a one step reaction. However, as illustrated in Fig. 6, distinctly non-linear Arrhenius plots result when methane is used as the substrate indicative of a reaction with two (or more) steps [25]. This may indicate that methane is oxidized by a unique mechanism. On the other hand, it may be that there is one mechanism with two steps for all substrates, but the steps are only similar in rate constant in the case of methane. We believe that the latter scenario is correct. If the two steps are assumed to be substrate binding and C–H bond breaking, either might

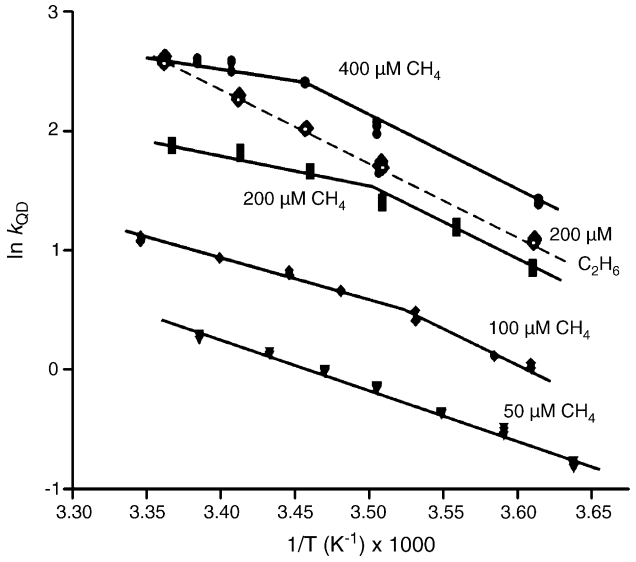

Fig. 6. Arrhenius plots for the Q decay reaction in the presence of methane or ethane. Adapted from [25], with permission.

be rate limiting in the temperature range accessible to stopped flow spectroscopy in aqueous media. If the rate-limiting step changes in this range for methane, then a break in the Arrhenius plot might be observed. For other substrates, with weaker C–H bonds, bond breaking might not become rate limiting in the relevant temperature range, so no break would be observed. Also, no KIE would be expected because only a small effect would be likely in the rate-limiting binding reaction. In the case of deuterated methane, the stronger C–H bond would make the bond-breaking reaction always rate limiting, so the Arrhenius plot would again be linear. A KIE would be observed because the C–H bond breaking reaction is rate limiting for both CH_4 and CD_4 over at least part of the observable temperature range.

The size of the KIE observed for methane raises an interesting question. This is clearly a non-classical KIE suggesting that the reaction proceeds with a significant contribution from quantum mechanical tunneling [25,40,41].

The strength of the C–H bond for methane and ethane suggests that the bond-breaking reaction may be rather slow. If this is the case, then the observation of a break in the Arrhenius plot for the methane reaction with Q suggests that the substrate binding reaction is also slow. This is unexpected because binding reactions of small molecules to enzymes usually approaches the diffusion-controlled limit. It seems likely that something impedes the binding process. This nature of the limiting factor can be reasonably proposed after studying the regulatory effects of MMOB in more detail.

2.5. The regulatory effects of MMOB

Chemical cross-linking and NMR relaxation studies have shown that a specific surface of MMOB forms a complex with the α-subunit of MMOH immediately above the active site pocket [42–46]. Because the NMR studies identified specific MMOB residues that contact the MMOH surface, site directed mutations could be made to explore their effects. It was found

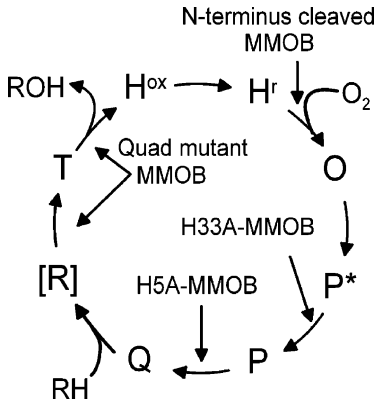

Fig. 7. Points in the MMOH catalytic cycle where the rate constant is affected by specific MMOB mutants. Adapted from [15], with permission.

that specific MMOB mutants affect the rate constants of specific steps in the MMOH catalytic cycle as illustrated in Fig. 7 [15]. For example, when the N-terminal 29 residues are removed, none of the steps in the cycle can be observed, due to a 1000-fold decrease in the key rate constant for the initial O_2 binding steps [44,47]. Site directed mutations of the two histidine residues in this N-terminal region were found to slow the rates of the two steps in the reaction cycle that require proton input, namely formation of P and of Q [15]. This suggests that these histidine residues may be part of the proton transport chain that connects the active site with the bulk solution. At the other end of MMOB, the carboxy-terminal region also dramatically affects rates in the reaction cycle. Deletion of as few as five residues from this region, causes the efficiency of hydroxylation by MMOH to substantially decrease such that some hydrogen peroxide is formed rather than hydroxylated product [48]. One cluster of four mutations termed the Quad mutant, and a derivative double mutation termed DBL2, affect the Q reaction and product release steps [15,40,41]. It was found that the reaction of Q with large substrates such as nitrobenzene or furan occurred up to seven times faster, while product release occurred twice as fast.

The increase in the rate constants for these substrate oxidation and product release steps in the cycle led to the hypothesis that MMOH acts effectively as a molecular sieve for methane (and O_2) [15]. As illustrated in Fig. 8 (also see Fig. 2), resting

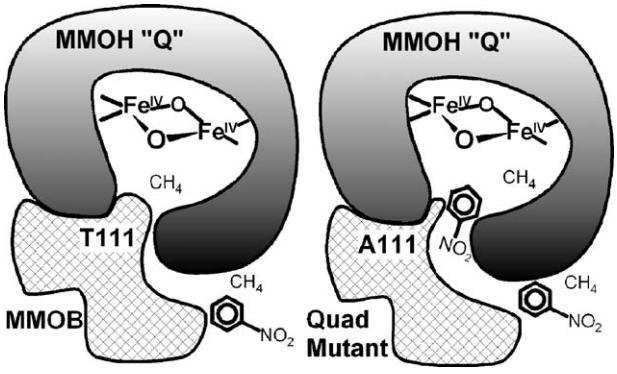

Fig. 8. Molecular sieve hypothesis for regulation of substrate binding to MMOH based on molecular size. MMOB is proposed to mediate this effect via residues near Thr111. Adapted from [15], with permission.

MMOH has a closed active site that would presumably greatly limit substrate binding. The MMOB complex appears to open a channel into the active site the size of methane. Consequently, methane is selected on the basis of size and larger substrates with weaker C–H bonds are partially excluded. This accounts for the apparent slow substrate binding suggested by the break in the Arrhenius plot for methane and provides a mechanism by which nature can selectively oxidize methane in the presence of other substrates.

Another informative observation is that methane reacts more slowly with Q when the Quad or DBL2 mutants are used [15,40,41]. This should not be related to the binding reaction since the mutants place smaller residues at the MMOH–MMOB interface which should open the putative channel wider. One possibility is suggested by the fact that the rate for CD_4 oxidation by Q is unaffected when the MMOB mutants are used. As a result, the KIE drops from 50 to 6, into the classical range. Thus, it may be that the ability of MMOH to catalyze the methane oxidation reaction by enhancing the quantum tunneling pathway is compromised in some way when MMOB is mutated [40,49]. This would presumably be related to the changes in MMOH active site structure caused by MMOB that are altered when a mutant is used.

Together these studies indicate that nature uses both size selection and the ability to design an active site that can promote quantum tunneling to make methane a better substrate for sMMO than other available molecules. These are functions of the protein structure removed from the metal ligands, but they are just as important to the function of the enzyme as the ability of the metal cluster to generate a dinuclear Fe(IV) intermediate. Notably, these features of the MMOH structure also make it very difficult to discern the chemical mechanism by diagnostic chemistry alone.

2.6. Defeating the regulatory mechanism

The MMOH compound Q reactions using the Quad and DBL2 MMOB mutants suggest that it is possible to perturb the regulatory mechanism. Indeed, for the ethane reaction with Q when the Quad mutant MMOB is used, a KIE of 2 is observed [49]. This is consistent with the enlarged channel allowing faster binding of ethane so that the binding rate constant becomes comparable with the C–H bond breaking constant. Similarly, the use of DBL2 results in a non-linear Arrhenius plot for the ethane reaction showing that the rate-limiting step now switches in the observable temperature range [41].

One quite informative MMOB mutant originated from an attempt to block the putative active site channel by introducing a larger tyrosine residue for the key residue of the Quad and DBL2 mutants, threonine 111. The T111Y mutant had the opposite of the expected effect by opening the channel to allow easy access by large substrates [40]. The reaction rate for ethane increased dramatically becoming almost diffusion controlled. We hypothesize that the large residue cannot be accommodated in the precisely structured interface, resulting in disruption of the MMOH structure and a new access route into the active site. Like the Quad and DBL2 mutants, the T111Y mutant also shows a greatly decreased KIE for the methane reaction. Thus, both restricted access and tunneling have apparently been defeated in this mutant. The result is that one can study the true reaction of Q with substrates for the first time. A plot of the log of the observed rate constant versus bond dissociation energy for methane, ethane and their deuterated adducts (calculated from zero point energies) shown in Fig. 9 appears linear when using this mutant. This plot is indicative of a hydrogen atom abstraction mechanism as proposed in the rebound mechanism (Fig. 5iii). Indeed, the slope of the plot is essentially the same as that for permanganate oxidation of arylalkanes, a known hydrogen atom abstraction reaction [50]. This type of reaction has been characterized in detail and a method to determine the energetics of the hydrogen atom abstracting species has been developed by Mayer and his colleagues [51]. In the case of Q, fissure of C–H bonds in the range of 105–110 kcal per mol is predicted from the reactions using the T111Y mutant.

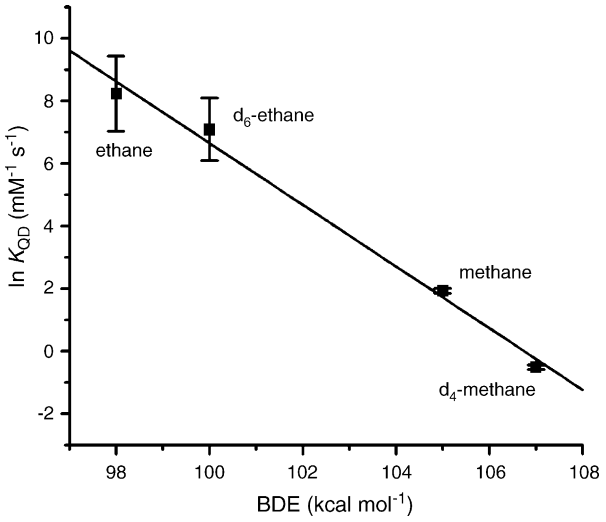

Fig. 9. Polanyi plot showing the relationship between the observed rate constant for Q decay and the bond dissociation energy of the C–H bond being cleaved. Adapted from [40], with permission.

2.7. Applications

An early goal of the sMMO studies was to develop a catalyst to produce methanol from natural gas. The difficulties of using a biological system for a high volume bulk process rapidly turned the goal toward using information gained from studying the sMMO mechanism to design small molecule catalysts, and this work continues. Other applications for sMMO as an environmental biodegradation reagent and as a tool for fine chemical synthesis are less affected by the limitations of a biological system, but they are hampered by the regulatory system of sMMO which favors methane. The studies reported here demonstrate that it is possible to modify the regulatory system so that larger substrates are readily oxidized. Further studies seem likely to lead to rules for tuning the stereo- and regio-selectivity as well, since these reaction properties are also controlled by MMOB [10].

3. Regulation of extradiol ring cleaving dioxygenases

Nature synthesizes and utilizes aromatic compounds in truly enormous quantities. For example, lignin, which is responsible for the rigid structure of plants, is composed of cross-linked aromatics. The biodegradation of lignin is a two-step process [52,53]. First, fungi produce extracellular peroxidase enzymes that diffuse radical species into the lignin mat, breaking it down into its component aromatics. Then, these aromatics are taken up by bacteria and the rings are opened, mainly by dioxygenase enzymes [54]. In this way, the bacteria can satisfy all of their carbon and energy needs.

The number and variety of enzymes that act in the entire set of aromatic functionalization, ring cleavage, and downstream pathway reactions is very great, but the key ring cleavage step is catalyzed by a few highly specific enzymes [53]. Generally, these enzyme require aromatic substrates that have two hydroxyl groups located either *ortho* (catechols) or *para* (gentisates) to one another. For the catechol group, ring cleavage can occur either between the hydroxyl functions (intradiol cleavage) or adjacent to one of the hydroxyls (extradiol cleavage). If there is a third substituent on the ring, the extradiol cleavage can be either proximal or distal relative to this substituent. Some examples of these cleavage patterns are given in Fig. 10.

Chemists have attempted to synthesize small molecule catalysts to mimic the reaction of each of these dioxygenase classes [see for example [4]]. The sheer volume of low cost raw materials and the utility of aliphatic straight chain building blocks that could be derived from aromatics after further processing (adipate, for example) make these catalysts valuable targets. A longstanding problem with the small molecule catalysts has been specificity. A good example is found in the efforts to mimic the reaction of extradiol dioxygenases using a metal ligand environment similar to that of the enzyme. The best metal-chelate models catalyze a high yield of the extradiol product, albeit at a fairly modest rate compared with that of the enzyme [55]. However, most models yield a mixture of extradiol and intradiol ring cleavage products along with a quinone oxidation product [56]. In contrast, the enzyme yields only the extradiol product with no detectible side products in any of the few hundred enzymes that are known in this class. We believe that the difference lies primarily in the structure of the second sphere surrounding the metal, but the studies described below also reveal a subtle interplay between the nature of the non-hydroxyl substrate substituents and the second sphere residues that finally determines the outcome of the reaction.

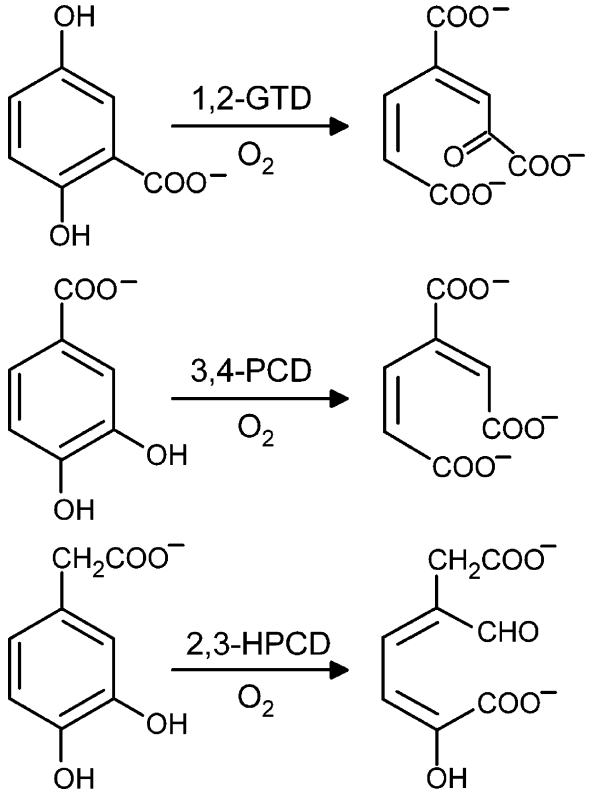

Fig. 10. Classes of dioxygenases illustrated from top to bottom by gentistate 1,2-dioxygenase, the intradiol cleaving protocatechuate 3,4-dioxygenase, and the proximal extradiol cleaving homoprotocatechuate 2,3-dioxygenase (HPCD).

3.1. The iron ligand environment of extradiol dioxygenases

Homoprotocatechuate 2,3-dioxygenase (HPCD) is a typical extradiol dioxygenase that catalyzes the insertion of both atoms of oxygen from O_2 into the aromatic ring of 3,4-dihydroxyphenyl acetate (HPCA) to yield the corresponding muconic semi-aldehyde (Fig. 10) [57]. This product is readily metabolized by bacteria to yield the fundamental molecules that support growth. The X-ray crystal structure of HPCD shows that the iron is bound by two histidines and one glutamic acid on one side of the coordination sphere, while three solvents occupy the other side [58]. This so-called 2-His-1-carboxylate facial triad motif illustrated in Fig. 11A was first recognized in the extradiol dioxygenase family [59,60], but now has been found in a remarkably broad range of enzymes [61]. It allows the enzyme to bind multiple substrates in a specific juxtaposition to the iron by displacing the solvents [62]. The iron serves to organize the substrates and to allow electron density to flow between them to promote catalysis.

The structural studies also show that the catecholic substrate binds as an asymmetric chelate to the iron; that is, the bond to one OH group is significantly longer than the other (Fig. 11B). We believe that this is due to the tendency of metal centers in enzymes to maintain a constant net charge [63]. In the case of HPCD, the iron is in the Fe(II) state and there is one anionic endogenous ligand and probably one anionic solvent ligand to neutralize the charge. When substrate binds, the anionic solvent serves to deprotonate one hydroxyl to maintain the charge, but there is no need to deprotonate the second hydroxyl. Consequently, it binds in the protonated state, lengthening the bond.

Following substrate chelation, a vacant site exists immediately next to the substrate. Structural studies in which NO is used as an oxygen surrogate indicate that O_2 binds in this vacant site to initiate the chemical reactions of ring cleavage [64].

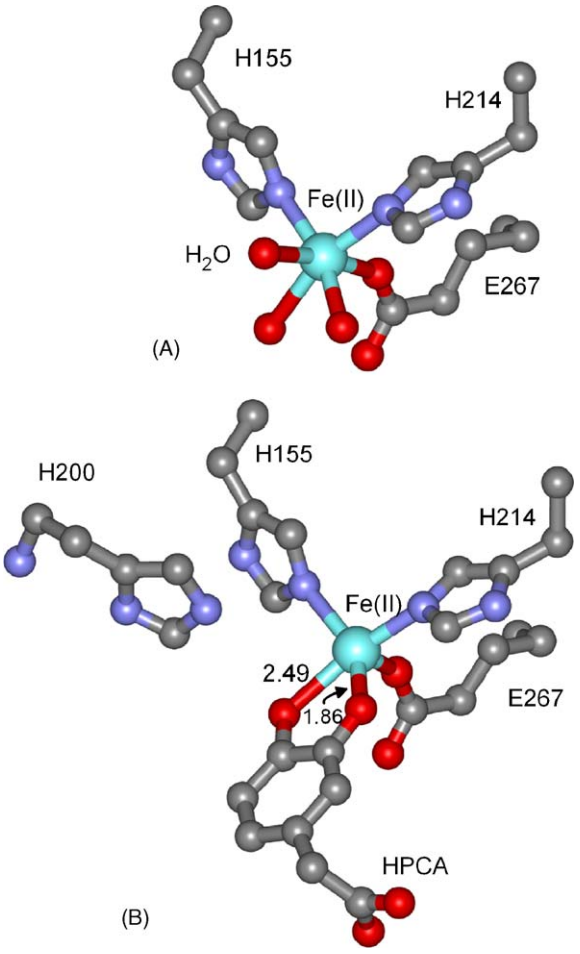

Fig. 11. Active site structure of HPCD. (A) Resting enzyme illustrating the 2-His-1-carboxylate facial triad (PDB 1F1X). (B) Anaerobic HPCA complex showing the orientation of His200 relative to the iron and substrate (PDB 1Q0C).

3.2. Steps in the catalytic cycle

As summarized in Fig. 12, we have speculated that the extradiol reaction proceeds by electron delocalization from the substrate via the iron to the oxygen to yield an iron-superoxo species [62,65]. Nucleophilic attack of this species on the substrate would yield a peroxo-intermediate. Criegee rearrangement of this species would result in concerted O–O bond cleavage and ring insertion of one oxygen atom to yield a lactone intermediate with the second oxygen atom retained on the iron as a hydroxide. Finally, hydrolysis of the lactone by the hydroxide would yield the ring open product and give the oxygen stoichiometry expected for a dioxygenase.

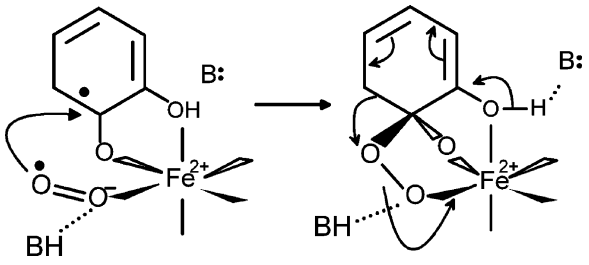

Fig. 12. Hypothesis for the oxygen activation and insertion steps in the extradiol dioxygenase mechanism.

It has been difficult to directly monitor the reaction to evaluate this mechanistic proposal because the Fe(II) is EPR silent and colorless, and no chromophoric intermediates are apparent prior to the ring opening step. The product itself is intensely yellow, so the point in the reaction where ring opening occurs is readily identified. Recently, we have approached this problem by using an alternative substrate, 4-nitrocatechol (4NC), which exhibits a chromophore that is sensitive to the ionization state of the hydroxyls and to its overall environment [57,63,66]. This allows the substrate-binding reaction to be monitored in real time. 4NC is cleaved in the proximal extradiol position like HPCA. The product is also high chromophoric, so this allows the ring cleavage step to be monitored. Thus, 4NC allows the entire reaction cycle to be observed for the first time in an extradiol dioxygenase. Using this approach, reaction cycle intermediates have been detected and rate constants determined for their interconversion.

The substrate binding reaction was characterized by reacting HPCD with an excess of 4NC under anaerobic conditions so that the reaction would halt before ring cleavage [63]. The kinetics of this process are complex, but the rate constants could be determined by multiple exponential fitting of time courses recorded for a variety of substrate concentrations and pH values. In contrast to HPCA, 4NC is a monoanion in solution at neutral pH. Deprotonation of the second OH group occurs during binding. This process occurs in several steps starting with 4NC monoanion binding to the enzyme, but not to the iron. Then, binding to the iron occurs and the second 4NC hydroxyl deprotonates. Finally, a structural rearrangement occurs to produce the final substrate complex we term E-4NC3. The kinetics show that, at neutral pH, two forms of the enzyme exist that are related by an ionization of an unknown group in the enzyme structure. One form reacts very slowly with substrate giving an extra phase in the kinetic time course.

The O_2 reaction phase of the cycle was studied by premixing HPCD and 4NC in a stoichiometric ratio at a concentration well above the dissociation constant for the complex. Adding an excess of O_2 allowed a pseudo first order reaction that stops after a single turnover to be observed. This reaction occurs in three observed steps with an unobserved O_2 binding step occurring at the start of the process. Ring cleavage occurs in the penultimate step followed by slow product release. Because there is no O_2 concentration dependence in any of the observed steps, the key oxygen binding and activation steps apparently occur too fast to detect. The complete catalytic cycle that can be postulated from these kinetic studies is shown in Fig. 13.

3.3. The role of the second sphere

Criegee rearrangement chemistry would be facilitated if electron density is pushed into the aromatic ring of the substrate and pulled out of the iron-bound proximal oxygen to promote O–O bond cleavage (see Fig. 12). The former will be affected by the nature of the aromatic ring substituents and possibly an active site base that would deprotonate the second OH group of HPCA.

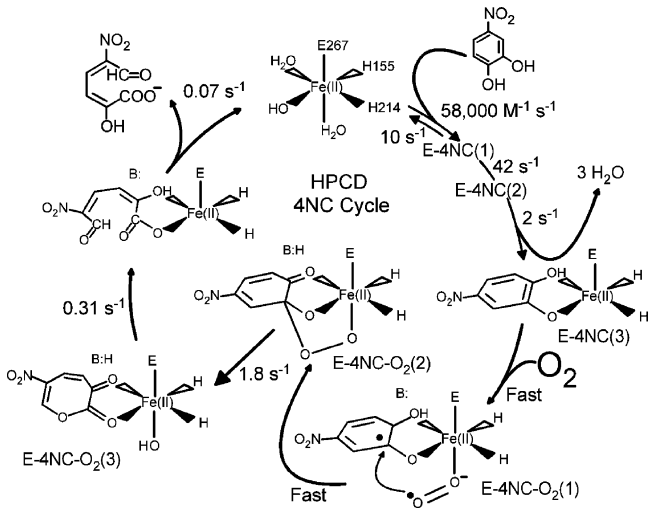

Fig. 13. Hypothesis for the complete catalytic cycle of HPCD using 4NC as the substrate.

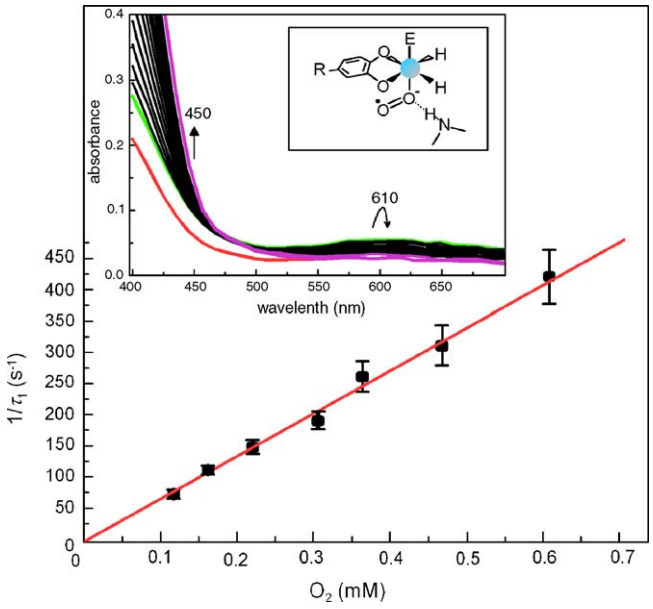

Fig. 14. Linear dependence on O_2 concentration of the rate constant for disappearance of the HPCD-substrate complex. HPCA is used as the substrate in the case shown, but similar results are found using 4NC. *Inset:* Rapid scan spectra of the development and decay of the oxy-intermediate and hypothesis for its structure. Arrows show the direction of absorbance change. Adapted from [66]. with permission.

The electron density on the proximal oxygen would be affected by hydrogen bonding or an active site acid that could protonate the oxygen as the O–O bond breaks. Inspection of the active site structure shows that there are several potential acid/base or hydrogen bonding residues near the substrate and O_2 binding sites on the metal. One residue, His200, is conserved throughout the extradiol dioxygenase family and is positioned just 4 Å from the iron near the O_2 and HPCA binding sites. We speculated that mutagenesis of His200 to a non-acid/base or non-hydrogen bonding residue might perturb the kinetics of the reaction cycle.

Mutation of His200 to residues that can neither hydrogen bond or catalyze acid/base chemistry resulted in 10–100-fold decrease in the turnover rate of HPCD [66]. In contrast, residues such as asparagine (H200N) that cannot participate in acid/base chemistry, but can hydrogen bond, caused only a 2–6-fold decrease in turnover number. Because the reaction cycle of extradiol dioxygenases is normally rate limited by product release, the changes observed in turnover number may not reflect the magnitude of the changes in rate constants for internal steps of the reaction cycle. To investigate this possibility, single turnover kinetics using 4NC was used to determine the effects on intermediate formation and interconversion.

The binding of 4NC to the H200X mutant enzymes occurs with only small changes in the rate constants of the individual steps [66]. Thus, it appears that H200 does not serve as the active site base needed to deprotonate substrate as it binds to the metal. This supports our earlier speculation that the solvent hydroxide anion bound in the coordination sphere serves this purpose.

Much larger changes are observed for the O_2 binding and ring cleavage portion of the reaction cycle. The overall rate of the reaction leading to product formation is greatly slowed for a mutant such as H200N. However, a new, very fast phase is observed immediately after O_2 addition, leading to a new intermediate [66]. The optical properties of the intermediate show that the aromatic ring has not been cleaved. As shown in Fig. 14, the observed pseudo first order rate constant for the intermediate formation is linearly dependent on O_2 concentration, suggesting that the actual O_2 binding step can be observed using this mutant.

The decay of the intermediate that forms is very slow, indicating that it is a semi-stable oxy-adduct. If this is the case, then it might be possible to observe it directly based on its own chromophore rather than relying on modification of the chromophore of 4NC. Many iron-superoxo or -peroxo species absorb in the 500–800 nm range [67]. Accordingly, a low extinction coefficient change occurring on the proper time scale was observed for the reaction using 4NC as the substrate.

Another approach to the observation of the new oxy-intermediate is to use the natural substrate HPCA. This molecule is colorless in the visible, potentially allowing the chromophore of the oxy-intermediate to be observed without a background absorbance. This proved be correct, and the spectrum of the species absorbing near 610 nm with an extinction coefficient of around 600 $cm^{-1}\,M^{-1}$ was detected as shown in Fig. 14, inset [66].

Following formation of the oxy-intermediate, a very slow conversion to product was observed using either 4NC or HPCA. The facts that the oxy-intermediate is greatly stabilized and that the product forming reaction is slow suggest that His200 plays two related roles. First, it promotes the reaction of the oxy-intermediate with substrate. Second, it appears to promote the Criegee rearrangement proposed to result in oxygen insertion and ring opening. A proposal for these roles in shown in Fig. 15.

3.4. The influence of the second sphere on specificity of product formation

The optical spectrum of the product formed as H200N catalyzes oxidation of 4NC is similar to that of the usual ring cleavage product, but not identical. Notably the characteristic

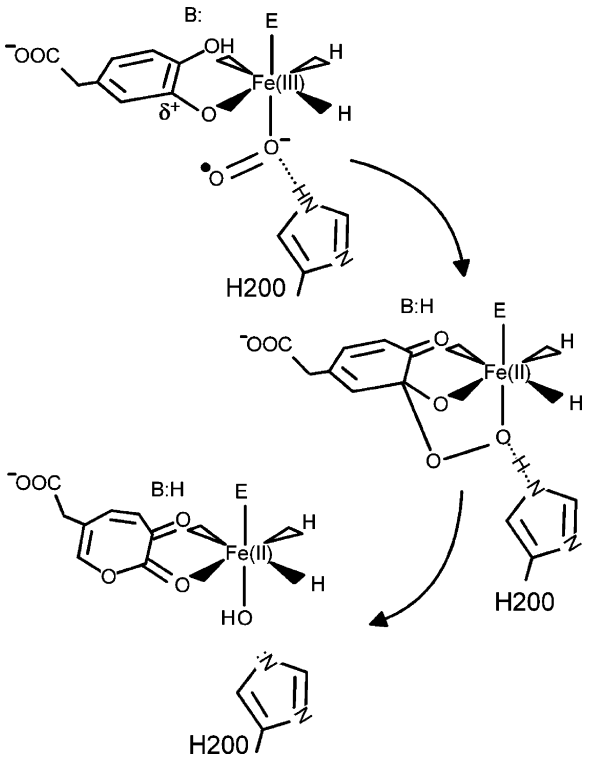

Fig. 15. Proposes roles for His200 in catalysis.

absorbance band at 330 nm is missing and the major absorbance band is shifted from 390 to 400 nm. These optical properties are those of the 4NC quinone [66]. Thus, the ring cleavage reaction is almost entirely eliminated by a change that does not involve the iron ligation. This is a very clear example of the influence of the second sphere residues and the importance of the presence of an acid catalyst at position 200 in HPCD. The modified reaction cycle of HPCD caused by the H200N mutation and the use of 4NC as the substrate are shown in Fig. 16. It appears that the ability to form the oxy-intermediate is retained, but the subsequent insertion reaction does not occur in accord with the roles for His200 illustrated in Fig. 15.

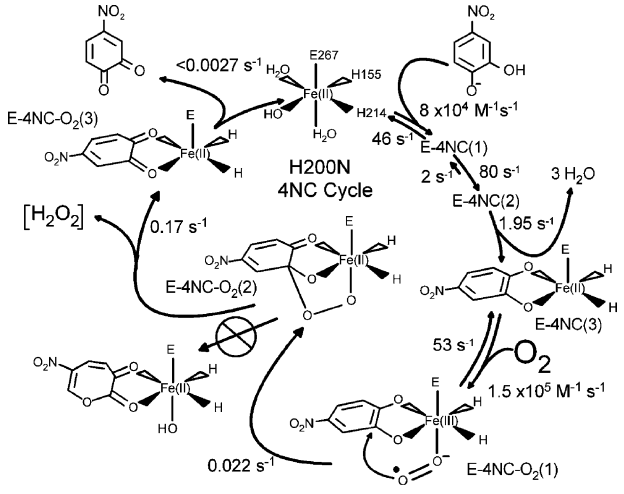

Fig. 16. Hypothesis for the complete catalytic cycle of the H200N mutant of HPCD using 4NC as the substrate. Adapted from [66], with permission.

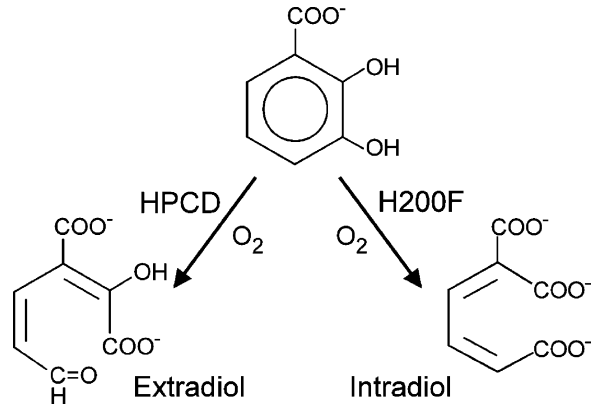

Fig. 17. HPCD can be switched from distal extradiol cleavage of 2,3-dihydroxybenzoate to intradiol cleavage by mutation of H200.

It is important to recognize that wild type HPCD promotes 100% proximal extradiol ring cleavage when 4NC is the substrate and H200N produces 100% proximal extradiol cleavage when HPCA is the substrate. Thus, the incorrect product is only found when both the critical acid catalyst is missing from the active site and the non-hydroxyl substrate substituent is altered. One way to rationalize this result is that the Criegee rearrangement works most efficiently when there is both a push of electron density into the aromatic ring and a pull of density from the oxygen, but only one of these effects may be sufficient to allow the reaction to proceed. Thus, substitution of a weakly electron donating acetyl group by a strongly electron withdrawing nitro group and replacement of an acid catalyst by a hydrogen bonding moiety changes the nature of the reaction, but ring cleavage still occurs when only one of these changes is made.

Another way to explore the influence of the second sphere and substrate substituents is to use substrates that make larger changes in substituent orientations. The reaction of 2,3-dihydroxbenzoate, in which the non-hydroxyl substituent is shortened and rotated one position on the ring, provides an informative example. Wild type HPCD turns over the substrate to yield extradiol cleavage, but it occurs in the distal position rather than the normal proximal position. When the His200 to phenylalanine mutant is used, the product is 2-carboxy muconic acid, which is the result of intradiol cleavage (Fig. 17) [68]. Thus, the combination of changes in the second sphere and to the substrate allow two more types of reactions from the same metal binding site.

Comparison of the reactions of the small molecule chelate catalysts designed to promote extradiol ring cleavage to those now observed for HPCD and its mutants shows that both systems exhibit the same range of chemistry. The difference is the ability of the wild type enzyme to select only one type of chemistry through control of the second sphere structure, which is clearly tuned to work with the specific substrate for which the enzyme evolved.

3.5. Applications

The important role played by the second sphere residues of an enzyme active site, as well as the significant effects of sub-

strate substituents, highlights two of the problems chemists face as they attempt to design small molecule catalysts to mimic the reactivity of aromatic ring cleaving dioxygenases. Nevertheless, knowledge of the function of specifically placed second sphere residues will aid in the development of such catalysts as synthetic techniques become more sophisticated. Indeed, some of the challenges set forth by nature, such as vacant coordination sites adjacent to substrate binding sites and asymmetric coordination spheres are now being mimicked successfully, and reactive second sphere residues have been built into small molecule catalysts in a few cases [4].

It was noted above that the direct application of methane monooxygenase to synthetic applications on a production scale is unlikely. This follows because three enzyme components are required, NADH is utilized in the oxygen activation process, and only half of the oxygen from O_2 is incorporated into the product. In contrast, the direct application of ring cleaving dioxygenase enzymes is more feasible. These are single component enzymes that are relatively robust. No cofactors from solution are required and both atoms of O_2 are incorporated into the final product. Now that we have reached a better understanding of the roles of the second sphere residues and other aspects of the active site from related studies, it should be possible to design catalysts to convert a wide variety of aromatic compounds to form targeted, stereospecific products in high yield.

Acknowledgment

This work was supported by National Institutes of Health Grants GM40466 and GM24689.

References

[1] R.H. Holm, P. Kennepohl, E.I. Solomon, Chem. Rev. 96 (1996) 2239.
[2] R.H. Holm, I. Solomon Edward, Chem. Rev. 104 (2004) 347.
[3] I.J. Higgins, D.J. Best, R.C. Hammond, Nature 286 (1980) 561.
[4] M. Costas, M. Mehn, P.M. Jensen, P.L. Que Jr., Chem. Rev. 104 (2004) 939.
[5] E.A. Lewis, W.B. Tolman, Chem. Rev. 104 (2004) 1047.
[6] B.J. Wallar, J.D. Lipscomb, Chem. Rev. 96 (1996) 2625.
[7] A.C. Rosenzweig, C.A. Frederick, S.J. Lippard, P. Nordlund, Nature 366 (1993) 537.
[8] N. Elango, R. Radhakrishnan, W.A. Froland, B.J. Wallar, C.A. Earhart, J.D. Lipscomb, D.H. Ohlendorf, Protein Sci. 6 (1997) 556.
[9] Y. Liu, J.C. Nesheim, S.-K. Lee, J.D. Lipscomb, J. Biol. Chem. 270 (1995) 24662.
[10] W.A. Froland, K.K. Andersson, S.-K. Lee, Y. Liu, J.D. Lipscomb, J. Biol. Chem. 267 (1992) 17588.
[11] S.C. Pulver, W.A. Froland, J.D. Lipscomb, E.I. Solomon, J. Am. Chem. Soc. 119 (1997) 387.
[12] K.E. Paulsen, Y. Liu, B.G. Fox, J.D. Lipscomb, E. Münck, M.T. Stankovich, Biochemistry 33 (1994) 713.
[13] H. Dalton, Adv. Appl. Microbiol. 26 (1980) 71.
[14] J. Colby, D.I. Stirling, H. Dalton, Biochem. J. 165 (1977) 395.
[15] B.J. Wallar, J.D. Lipscomb, Biochemistry 40 (2001) 2220.
[16] B.G. Fox, J.G. Borneman, L.P. Wackett, J.D. Lipscomb, Biochemistry 29 (1990) 6419.
[17] J.P. Sullivan, D. Dickinson, H.A. Chase, Crit. Rev. Microbiol. 24 (1998) 335.
[18] N.D. Priestley, H.G. Floss, W.A. Froland, J.D. Lipscomb, P.G. Williams, H. Morimoto, J. Am. Chem. Soc. 114 (1992) 7561.
[19] F. Ruzicka, D.S. Huang, M.I. Donnelly, P.A. Frey, Biochemistry 29 (1990) 1696.
[20] Y. Jin, J.D. Lipscomb, Biochim. Biophys. Acta 1543 (2000) 47.
[21] B.J. Brazeau, R.N. Austin, C. Tarr, J.T. Groves, J.D. Lipscomb, J. Am. Chem. Soc. 123 (2001) 11831.
[22] A.M. Valentine, M.-H. LeTadic-Biadatti, P.H. Toy, M. Newcomb, S.J. Lippard, J. Biol. Chem. 274 (1999) 10771.
[23] B.G. Fox, W.A. Froland, J.E. Dege, J.D. Lipscomb, J. Biol. Chem. 264 (1989) 10023.
[24] S.-K. Lee, J.C. Nesheim, J.D. Lipscomb, J. Biol. Chem. 268 (1993) 21569.
[25] B.J. Brazeau, J.D. Lipscomb, Biochemistry 39 (2000) 13503.
[26] S.-K. Lee, J.D. Lipscomb, Biochemistry 38 (1999) 4423.
[27] K.E. Liu, A.M. Valentine, D. Qiu, D.E. Edmondson, E.H. Appelman, T.G. Spiro, S.J. Lippard, J. Am. Chem. Soc. 117 (1995) 4997.
[28] M. Costas, J.-U. Rohde, A. Stubna, R.Y.N. Ho, L. Quaroni, E. Münck, L. Que Jr., J. Am. Chem. Soc. 123 (2001) 12931.
[29] T.J. McMurry, J.T. Groves, in: P.R. Ortiz de Montellano (Ed.), Cytochrome P-450 Structure, Mechanism, and Biochemistry, Plenum Press, New York, 1986, p. 1.
[30] I. Schlichting, J. Berendzen, K. Chu, A.M. Stock, S.A. Maves, D.E. Benson, R.M. Sweet, D. Ringe, G.A. Petsko, S.G. Sligar, Science 287 (2000) 1615.
[31] S.-K. Lee, B.G. Fox, W.A. Froland, J.D. Lipscomb, E. Münck, J. Am. Chem. Soc. 115 (1993) 6450.
[32] L. Shu, J.C. Nesheim, K. Kauffmann, E. Münck, J.D. Lipscomb, L. Que Jr., Science 275 (1997) 515.
[33] A.L. Feig, S.J. Lippard, Chem. Rev. 94 (1994) 759.
[34] B.F. Gherman, S.J. Lippard, R.A. Friesner, J. Am. Chem. Soc. 127 (2005) 1025.
[35] K. Yoshizawa, T. Yumura, Chem. Eur. J. 9 (2003) 2347.
[36] S.-Y. Choi, P.E. Eaton, D.A. Kopp, S.J. Lippard, M. Newcomb, R. Shen, J. Am. Chem. Soc. 121 (1999) 12198.
[37] Y. Jin, J.D. Lipscomb, Biochemistry 38 (1999) 6178.
[38] Y. Jin, J.D. Lipscomb, J. Biol. Inorg. Chem. 6 (2001) 717.
[39] J.C. Nesheim, J.D. Lipscomb, Biochemistry 35 (1996) 10240.
[40] B.J. Brazeau, J.D. Lipscomb, Biochemistry 42 (2003) 5618.
[41] H. Zheng, J.D. Lipscomb, Biochemistry 45 (2006) 1685.
[42] B.G. Fox, Y. Liu, J.E. Dege, J.D. Lipscomb, J. Biol. Chem. 266 (1991) 540.
[43] S.L. Chang, B.J. Wallar, J.D. Lipscomb, K.H. Mayo, Biochemistry 38 (1999) 5799.
[44] S.L. Chang, B.J. Wallar, J.D. Lipscomb, K.H. Mayo, Biochemistry 40 (2001) 9539.
[45] K.J. Walters, G.T. Gassner, S.J. Lippard, G. Wagner, Proc. Natl. Acad. Sci. U.S.A. 96 (1999) 7877.
[46] B.J. Brazeau, B.J. Wallar, J.D. Lipscomb, Biochem. Biophys. Res. Commun. 312 (2003) 143.
[47] A.J. Callaghan, T.J. Smith, S.E. Slade, H. Dalton, Eur. J. Biochem. 269 (2002) 1835.
[48] J. Zhang, J.D. Lipscomb, Biochemistry 45 (2006) 1459.
[49] B.J. Brazeau, B.J. Wallar, J.D. Lipscomb, J. Am. Chem. Soc. 123 (2001) 10421.
[50] K.A. Gardner, L.L. Kuehnert, J.M. Mayer, Inorg. Chem. 36 (1997) 2069.
[51] J.P. Roth, J.C. Yoder, T.-J. Won, J.M. Mayer, Science 294 (2001) 2524.
[52] T.K. Kirk, in: D.T. Gibson (Ed.), Microbial Degradation of Organic Compounds, Marcel Dekker Inc., New York, 1984, p. 399.
[53] J.D. Lipscomb, A.M. Orville, in: H. Sigel, I. Sigel (Eds.), Metal Ions in Biological Systems, Marcel Dekker, New York, 1992, p. 243.
[54] S. Dagley, in: J.R. Sokatch (Ed.), The Bacteria, Academic Press, New York, NY, 1986, p. 527.
[55] M. Ito, L. Que Jr., Angew. Chem. Int. Ed. Engl. 36 (1997) 1342.
[56] M.G. Weller, U. Weser, J. Am. Chem. Soc. 104 (1982) 3752.
[57] M.A. Miller, J.D. Lipscomb, J. Biol. Chem. 271 (1996) 5524.

[58] M.W. Vetting, L.P. Wackett, L. Que Jr., J.D. Lipscomb, D.H. Ohlendorf, J. Bacteriol. 186 (2004) 1945.
[59] S. Han, L.D. Eltis, K.N. Timmis, S.W. Muchmore, J.T. Bolin, Science 270 (1995) 976.
[60] K. Sugiyama, T. Senda, H. Narita, T. Yamamoto, K. Kimbara, M. Fukuda, K. Yano, Y. Mitsui, Proc. Jpn. Acad. Ser. B Phys. Biol. Sci. 71 (1995) 32.
[61] E.L. Hegg, L. Que Jr., Eur. J. Biochem. 250 (1997) 625.
[62] D.M. Arciero, J.D. Lipscomb, J. Biol. Chem. 261 (1986) 2170.
[63] S.L. Groce, M.A. Miller-Rodeberg, J.D. Lipscomb, Biochemistry 43 (2004) 15141.
[64] N. Sato, Y. Uragami, T. Nishizaki, Y. Takahashi, G. Sazaki, K. Sugimoto, T. Nonaka, E. Masai, M. Fukuda, T. Senda, J. Mol. Biol. 321 (2002) 621.
[65] L. Shu, Y.-M. Chiou, A.M. Orville, M.A. Miller, J.D. Lipscomb, L. Que Jr., Biochemistry 34 (1995) 6649.
[66] S.L. Groce, J.D. Lipscomb, Biochemistry 44 (2005) 7175.
[67] G. Roelfes, V. Vrajmasu, K. Chen, R.Y.N. Ho, J.-U. Rohde, C. Zondervan, R.M. la Crois, E.P. Schudde, M. Lutz, A.L. Spek, R. Hage, B.L. Feringa, E. Münck, L. Que Jr., Inorg. Chem. 42 (2003) 2639.
[68] S.L. Groce, J.D. Lipscomb, J. Am. Chem. Soc. 125 (2003) 11780.